Results in Physics 23 (2021) 103986

Contents lists available at ScienceDirect

Results in Physics

journal homepage: www.elsevier.com/locate/rinp

Graphene-assisted infrared plasmonic metamaterial absorber for gas detection

Yashar E. Monfared [a,*], Montasir Qasymeh [b]

[a] Department of Chemistry, Dalhousie University, 6274 Coburg Road, Halifax, Nova Scotia, Canada
[b] Department of Electrical and Computer Engineering, Abu Dhabi University, United Arab Emirates

ARTICLE INFO

Keywords:
Gas sensor
Plasmonic metamaterial
Graphene plasmonics
Refractive index sensor

ABSTRACT

In this paper, we propose a graphene-assisted plasmonic metamaterial absorber to operate as an ultra-compact optical gas sensor in the infrared (IR) region. The metamaterial absorber is comprised of a thin silicon-dioxide layer that is middling between a gold film and an array of graphene-coated gold nano-disks. Using the finite element method, we investigate the resonance characteristics of the proposed plasmonic metamaterial and show that the metamaterial has three distinct resonances in visible and infrared regions. We demonstrate that the strongest absorption peak of the proposed metamaterial is attributed to a fundamental localized surface plasmon resonance in IR, which has also the highest spectral sensitivity to the refractive index (RI) variations of the surrounding medium. The sensing mechanism is based on evaluation of gaseous medium RI surrounding the nano-disks, by illuminating the metamaterial with IR radiation and subsequently measuring the reflection or absorption spectra of the structure. We show that graphene coating of the gold nano-disks improves the sensitivity of the metamaterial to the gas RI by more than two times. Using the optimized design parameters, an average linear spectral sensitivity of 720 nm/RIU and an approximate detection limit of 1×10^{-5} RIU has been obtained for gas RI variations between 1 and 1.05. We also show that the proposed sensor has a linear response even for extremely small variations in gas RI in the order of 10^{-5} RIU. The proposed metamaterial configuration is relatively easy to fabricate and can be used to monitor low concentrations of various gases in different applications ranging from environmental monitoring to home safety monitoring systems.

Introduction

Monitoring the presence (or the concentration) of gases is of particular interest in various applications ranging from monitoring environments to home safety systems [1]. For example, accurate measurement of CO_2 gas concentration in the atmosphere is important for studying the cascading effects of global warming [1,2]. Therefore, there is a growing need for compact and accurate CO_2 gas sensors that can be efficiently deployed in wide area sensor networks to monitor trends in greenhouse gas concentrations [2]. Gas sensors with high sensitivity, small size and simple design can also be used for monitoring air quality in real time [3]. Another strong interest in gas monitoring arises in the field of health sciences since gases plays an important role in many biological activities [4]. One of the most common gas detection technologies is resistive gas sensing which usually suffer from the long warm-up time in order to react with the target gas at the sensing surface [5,6]. This problem restricts application of this detection technology due to the high-power consumption of the heater as well as the long warm-up time [5,6].

Recent advances in optical gas sensors provide a path for miniaturized, accurate, and real-time monitoring of gas concentrations in various environments [6,7]. The optical gas sensors are usually based on measuring the reflection, transmission, or absorption of the intensity of a light beam subjected to a medium containing gas [6,7]. One of the most interesting candidates for optical sensing in gaseous media is plasmonic-based or surface plasmon resonance (SPR) based sensors which detects the changes in refractive index of gases by monitoring the light transmission, reflection or absorption [7]. SPR is an important optical phenomenon that involves a transfer of energy from the incident propagating light to a surface plasmon mode under resonance conditions [8–11]. Surface plasmon is a form of collective electron oscillations at the interface between a dielectric and a metal [8–11]. The surface plasmons can be generated by nano-particles, nano-films, or nano-gratings or an array of nano-structured thin films. As the excitation of

* Corresponding author.
E-mail address: y.monfared@dal.ca (Y.E. Monfared).

https://doi.org/10.1016/j.rinp.2021.103986
Received 17 January 2021; Received in revised form 10 February 2021; Accepted 11 February 2021
Available online 25 February 2021

surface plasmons and their resonance condition strongly depend on the nearby environment, SPR-based devices are capable to detect ultra-small changes in the refractive indices of surrounding liquids [8,9] or gases [7].

There are different plasmonic sensing platforms which have been used for gas sensing applications. These include the prism-based plasmonic sensors, which are implemented either with Otto configuration or Kretshmann configurations [12], and the grating-based plasmonic sensors [6]. From practical point of view, the prism-based setups (Kretschmann and Otto configurations) are not suitable for many real-world applications as they are bulky, and thus, they cannot satisfy the small probe size requirement for the on-chip integration which is usually needed for gas sensors [8]. While the grating-based plasmonic devices show great potential for the on-chip realization and small probe size, their sensitivity and detection limit are usually not large enough to detect low gas concentration [6]. In addition, as these conventional plasmonic devices are based on noble metals like gold (Au) and silver (Ag), the response of these sensors is usually limited to the visible range [8–10]. However, infrared (IR) region is particularly interesting for gas sensing application since IR spectra is conceived as molecular fingerprint region of many gases [13]. One of the most efficient ways to design sensitive IR-based plasmonic gas sensor with small size and high accuracy is to use metamaterials.

Metamaterials are artificially engineered and periodically arranged nanostructures that possess unusual electromagnetic properties that are not found in natural materials [14–16]. By properly tailoring the geometrical dimensions of metamaterials, the electromagnetic responses of the metamaterial-based devices can be realized in microwave, terahertz (THz), infrared (IR), visible and ultraviolet (UV) spectra ranges [17–19]. Combining metamaterials with surface plasmons provide new type of metamaterials, termed as plasmonic metamaterials, which are governed by the interaction of the incident electromagnetic waves with the metal–insulator interfaces [14,15]. The simplest and easiest geometry of plasmonic metamaterials to fabricate is the metal–insulator–metal (MIM) structure which is usually based on combination of noble metals, like Au and Ag, and insulator material like SiO_2 or Al_2O_3 [15,16].

The sensitivity levels and the detection range as well as tunability of the plasmonic metamaterial sensors can be further enhanced by utilizing graphene in the sensor structure [20,21]. Graphene can offer improved sensitivity besides providing surface protection as a coating layer for the metal plasmonic films [21]. Here, we propose a highly sensitive IR gas sensor based on a graphene-assisted plasmonic MIM configuration. Our sensor can overcome the limitation of the conventional plasmonic gas sensors by increasing the detection limit and detection range yet using simple configuration. These combined advantages open up new horizons for low-cost, real-time and label-free optical gas sensing as compared with conventional cumbersome methods like fluorescence detection or resistive gas sensing.

Design, materials, and methods

In order to detect variations in the refractive index of gases, one can design a plasmonic sensor using a combination of plasmonic nano-antennas (i.e., nano-disks, nano-gratings, nano-films) with dielectric layers. As excitation of surface plasmons at the interface between nano-antennas and dielectric medium strongly depend on the RI of media surrounding the nano-antennas (i.e., gaseous medium), the structure can operate as a RI sensor. Here, we first specify the design parameters of the metamaterial and then analyze the absorption properties of our proposed metamaterial absorber. We then study the gas sensing performance of our device in the final section. The schematic of the proposed graphene-assisted metamaterial absorber irradiated with a broadband light source together with the geometry of the metamaterial unit cell are depicted in Fig. 1a and b, respectively.

The metamaterial is composed of periodic gold (Au) disk-shape nanoantenna array, and a continuous Au film which is separated from nano-antennas by a silicon dioxide (SiO_2) dielectric layer. The topmost disk nano-antennas are periodically distributed in both the x- and y-directions with a gap size of g = 300 nm. In the unit cells, the diameter and the thickness of the disk nano-antennas are d = 300 nm and $t_d = 10$ nm, respectively. Au nano-disks are coated with a single graphene layer ($t_{graphene} = \Delta = 0.34$ nm) to induce resonance tunability, increase the surface stability of the nano-disks, and improve absorption sensitivity of the metamaterial to the changes in surrounding environment. The thickness of the middle SiO_2 spacer layer is optimized to be $t_{si} = 30$ nm, and the bottom Au layer has a thickness of $t_{au} = 100$ nm, which is thick enough to block almost all the transmission in the investigated wavelength range. In the unit cells, the Au and SiO_2 layers have the same width and length of $W = L = 600$ nm. In the presented simulations, we used three dimensional (3D) full-wave simulations to verify the performance of the graphene-assisted metamaterial. The full-wave simulations

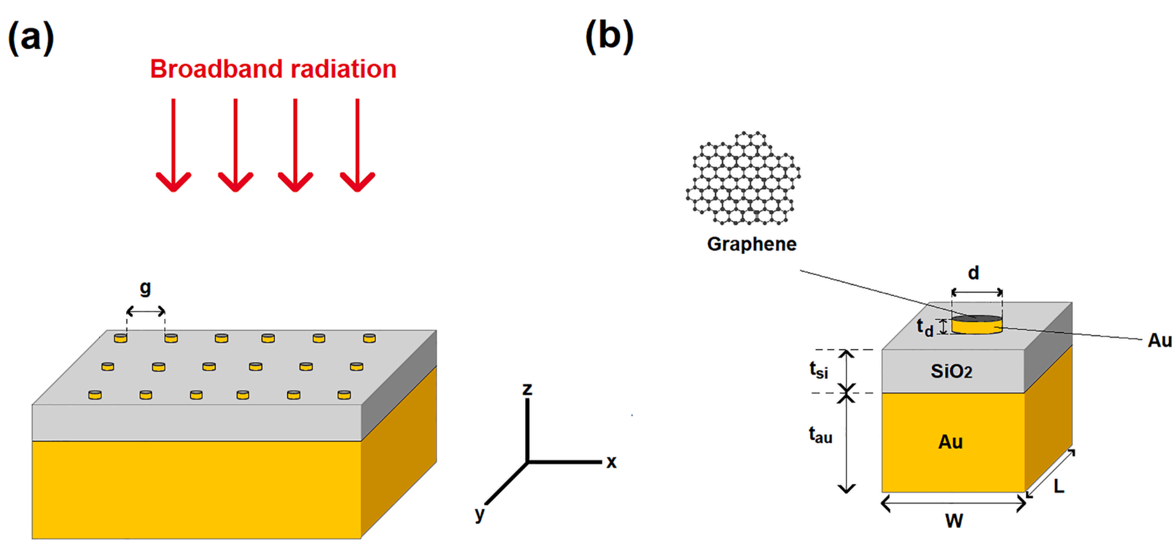

Fig. 1. (a) Schematic of the proposed graphene-assisted metamaterial absorber irradiated with a broadband light source with nano-disks gap size *g*, and (b) The geometry of the metamaterial unit cell with the following design parameters: nano-disk diameter d, unit cell width *W*, unit cell length *L*, thickness of Au nano-disks t_d, thickness of SiO_2 nano-film t_{si} and thickness of Au nano-film t_{au}.

are performed using the finite element method (FEM) applied with COMSOL Multiphysics software. In the simulations, we modeled a single unit cell by applying periodic boundary conditions on the vertical sides of the cell which mimic the results for the whole periodic structure. The incident wave is assumed to be a plane wave propagating normal to the surface. In the Au-SiO_2-Au-graphene configuration, the complex permittivity of Au is obtained from the previous experimental data [22].

In our simulations, we consider material dispersion of SiO_2 to accurately simulate the resulting structure. Relationship between the refractive index of SiO_2 and incident light wavelength is given by the following Sellmeier's equation [23]:

$$n_{SiO2}^2 = 1 + \frac{0.6961663\lambda^2}{\lambda^2 - 0.0684043^2} + \frac{0.4079426\lambda^2}{\lambda^2 - 0.1162414^2} + \frac{0.8974794\lambda^2}{\lambda^2 - 9.896161^2}, \quad (1)$$

where λ is the wavelength of incident light. In this work, the graphene layer is modeled as an ultrathin layer material with thickness Δ and effective bulk permittivity ε_{eff}. The graphene effective permittivity used in our simulations is given by [24]:

$$\epsilon_{eff} = \epsilon_0 - \frac{Im(\sigma_s)}{\omega\Delta} + i\frac{Re(\sigma_s)}{\omega\Delta}, \quad (2)$$

where $\omega = 2\pi f$, and ε_0 is the permittivity of the free space, Δ is the graphene layer thickness (considered to be 0.34 nm) and σ_s is the graphene conductivity, given by [24]:

$$\sigma_s = \frac{iq^2}{4\pi\hbar} ln\left(\frac{2\mu_c - (f + i\tau^{-1})\hbar}{2\mu_c + (f + i\tau^{-1})\hbar}\right) + \frac{iq^2 K_B T}{\pi\hbar^2 (f + i\tau^{-1})}\left(\frac{\mu_c}{K_B T} + 2ln\left(e^{-\frac{\mu_c}{K_B T}} + 1\right)\right), \quad (3)$$

Here, the first term describes the interband conductivity, the second term represents the intraband conductivity, q is the electron charge, ħ is the reduced plank's constant, τ expresses the scattering relaxation time, K_B represents the Boltzman constant, T is the temperature which is considered to be 300 K, f is the frequency, and μ_c expresses the graphene chemical potential which is considered to be 0.3 eV. The medium around the metamaterial structure is chosen to be the air or gas (sample).

Results and discussions

Absorption properties

The transmission, reflection and absorption spectra of the proposed metamaterial have been calculated via FEM simulations in Fig. 2 from 600 nm to 2200 nm. We consider the ambient medium to be air with a refractive index of 1, and apply a y-polarized excitation normal to the surface of the metamaterial. We first analyze the light reflection and transmission from the metamaterial in Fig. 2a. As expected, there is nearly zero power transmission through the metamaterial in IR region due to relatively thick (100 nm) Au film at the bottom of the structure.

While it is possible to completely eliminate the transmission in IR region by further increasing the Au thickness, the transmission magnitude of the proposed metamaterial with 100 nm thickness of Au nanofilm in IR region ($\lambda > 1000$ nm) is still negligible (less than 0.02 compared to a peak value of 0.972 for absorption). Even in the visible region, the transmission is less than 0.04 which means one can obtain absorption spectra of the proposed metamaterial by simply measuring the light reflection in the experiments. Thus, we consider the Au film with 100 nm thickness in our simulations to reduce the cost and physical size of the absorber. In our FEM simulations, we considered the effect of weak transmission and calculated absorbance (A) using both reflectance (R) and transmittance (T) from the following relationship: A = 1 – R – T. The calculated absorption spectrum of graphene-assisted metamaterial is demonstrated in Fig. 2b. It be seen that the graphene-assisted metamaterial has two distinct resonances (absorption peaks) in the visible region at R_1 = 664 nm and R_2 = 737 nm and one resonance in the IR region at R_3 = 1753 nm. The first resonance in the visible region (R_1) has the smallest full-width at half maximum (FWHM) followed by R_2 and R_3 peaks. Furthermore, the peak in the IR region (R_3) has the largest absorption magnitude (A_{R3} = 0.972) compared to R_1 (A_{R1} = 0.275) and R_2 (A_{R2} = 0.190).

To analyze the effect of graphene coating of the nano-disks, we also compared the absorption of the metamaterial without graphene coating in Fig. 3. According to the data, graphene coating of Au nano-disks changes the dynamics of the metamaterial absorber. We observe a redshift of the absorption peak for all three resonances (R_1, R_2 and R_3) and a slight reduction in the peak FWHM after adding graphene coating to the Au nano-disks. Furthermore, our extensive numerical simulations demonstrate that graphene-coated nano-disks are more sensitive to variations in the medium RI that is close to metamaterial surface. The lower peak FWHM as well as the increased sensitivities can result in better sensing performance for the metamaterial, as will be discussed in section 3.3. This improvement in the absorption properties in both visible and IR region could be attributed to the lower optical loss of graphene-Au hybrid nanostructure compared to Au nano-disks.

Resonance characterization

To reveal the physical mechanism of the absorption in the proposed metamaterial, we calculated the electric and magnetic field profiles at the three absorption peak positions. Fig. 4 show the normalized electric

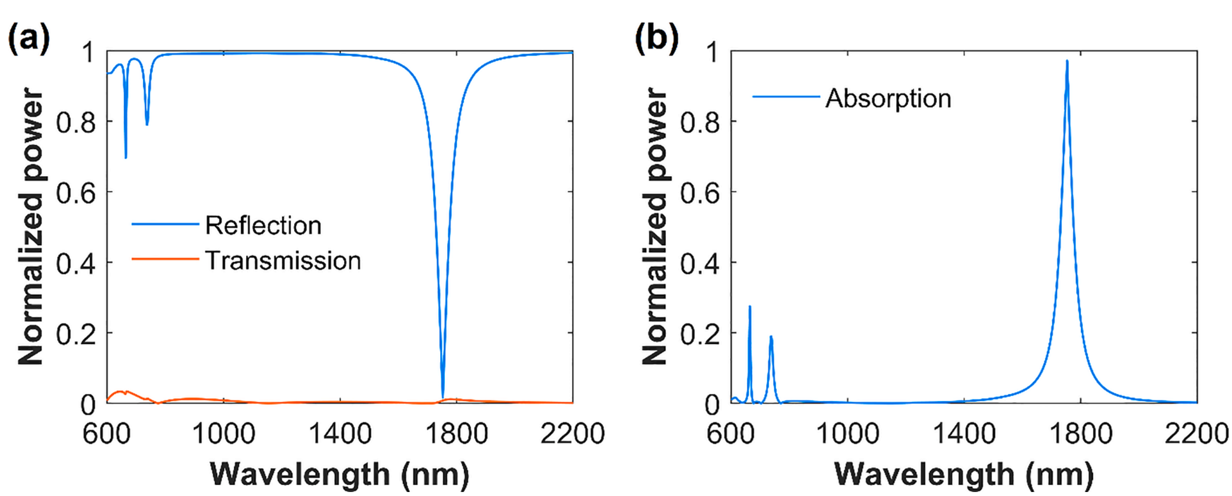

Fig. 2. (a) Transmission and reflection spectra of the proposed graphene-assisted metamaterial absorber. (b) Normalized absorption of the proposed metamaterial absorber with and without graphene coating of Au nano-disks.

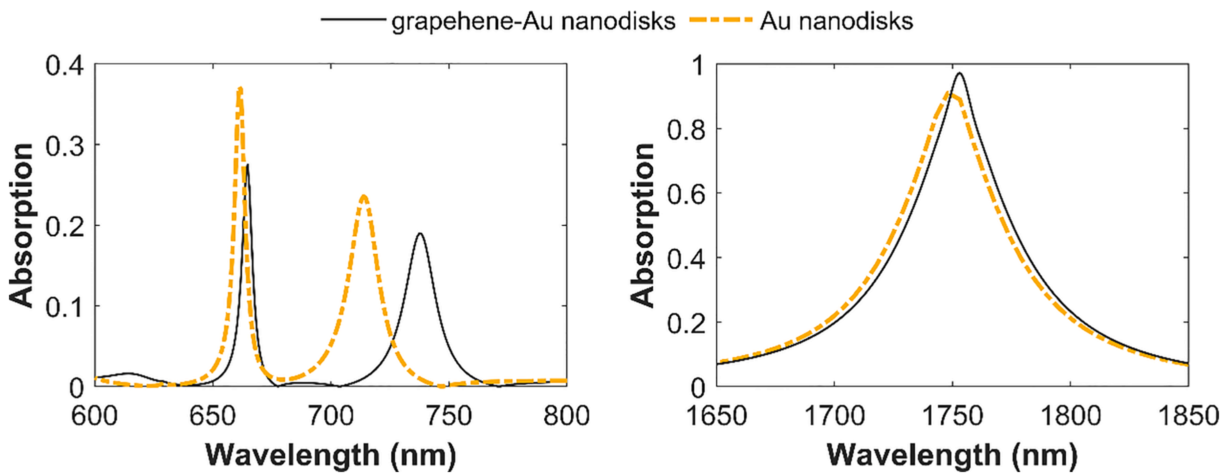

Fig. 3. Absorption of the proposed metamaterial absorber with and without graphene coating of Au nano-disks in (a) visible region, and (b) IR region.

(|Ey|) and magnetic (|Hx|) field distributions for different resonances (R_1, R_2 and R_3) in y-z and x-y planes. The resonances are essentially electric dipole resonances excited on the nano-disks along the x and y axes.

The short wavelength resonance at R_1 is considered to be hybrid mode which involves surface plasmon polariton (SPP) resonance between the continuous Au film and the SiO_2 layer, and localized surface plasmon resonance (LSPR) of the nano-disks. This can be inferred as the magnetic field is not only confined in the gap region underneath the nano-disks, but also strongly enhanced between the nano-disks. The modes at R_2 and R_3 are localized surface plasmon resonances (LSPRs) where the magnetic field is mainly concentrated within the gap between the topmost graphene-assisted nano-antennas and the gold nanofilm. The peak at R_3 is a fundamental LSPR since the magnetic field is completely confined in the intermediate dielectric layer effectively and there is no coupling between adjacent nano-disks.

As explained above, the main reason for observing three peaks in visible and IR regions in the absorption spectra of the structure is having different resonance/absorption mechanisms in the proposed metamaterial (hybrid SPP/LSPR, higher order LSPR mode, and fundamental LSPR mode, respectively). According to the data, most of the light energy will be absorbed by the strong fundamental localized resonance at R_3 in IR region, while a small portion of light energy can also be absorbed by higher order LSPR and hybrid SPP/LSPR mode at R_1 and R_2 in visible range. It should be noted that the graphene-assisted Au nanodisks dominate the total absorption in the IR region. The absorption of Au film at the bottom of the metamaterial is negligible for $\lambda > 1000$ nm which indicates that the Au substrate mainly works as a mirror to reflect the light energy in these spectral regions and contributes little to the direct absorption of the incident light. In the visible wavelength range where λ less than 700 nm, the Au layer can directly dissipate some of the incident energy which is in turn attributed to the generated (dominating) hybrid SPP-LSPR resonance at R_1. In this paper we will study the sensing performance of the proposed metamaterial absorber based on variations in peak location of R_3. While R_1 also demonstrate large sensitivity to variations in medium RI, we chose R_3 for RI sensing purposes. The main reasons for choosing R_3 over R_1 include the strong linearity, large absorption magnitude, and the possibility of having larger detection range of this LSPR resonance (R_3) compared to hybrid SPP-LSPR resonance (R_1).

The role of design parameters

The design parameters in this paper are optimized upon conducting extensive numerical investigations to maximize the RI sensitivity. Here, we also included our studies on the role of design parameters on the absorption spectra around LSPR in IR region (R_3) of the proposed sensor in Fig. 5. The design parameters studied in Fig. 5 has been chosen as larger and/or smaller values compared to our optimized values to demonstrate the contrast between absorption properties depending on the design parameters. Our extensive numerical simulations demonstrate that the dimensions of the nano-disks and the SiO_2 film are the deciding parameters on the absorption spectral properties among all other geometrical parameters. In particular, the variations in the width and length of the metamaterial unit cell (W and L) does not directly affect the sensitivities, for a given relative dimensions of the nano-disks and the gold/silica films (i.e., nano-disks gap size).

First, we studied the role of nano-disks diameter on the absorption properties of the metamaterial. According to the data and as the nano-disks diameter is increased from 200 nm to 400 nm in Fig. 5a, the resonance wavelength (R_3) redshifts significantly from 1517 nm to 1991 nm. It should be noted that the maximum absorption and lowest peak full-width at half maximum (FWHM), which leads to maximum sensing figure of merit (FOM), take place when $d = 300$ nm (the optimized value in our simulations).

The role of the thickness of SiO_2 nano-film is also studied in Fig. 5b. By increasing the thickness of SiO_2 layer from 20 nm to 40 nm, the resonance wavelengths blueshifts significantly from 1953 nm to 1651 nm. The maximum absorption and the lowest FWHM take place at $t_{si} =$ 30 nm which is the optimized design parameter in our studies. Different thickness of the nano-disks also results on changing the dynamics of the absorption in the proposed metamaterial, as demonstrated in Fig. 5c. By increasing the thickness of the nano-disks, the resonance wavelength blueshifts and dampens significantly. At larger thicknesses, the LSPR resonance in IR region (R_3) can be significantly damped and almost disappear.

It should be noted that the variations in the design parameters can not only change the absorption peak location, magnitude and broadness, but also can slightly modify the sensitivity of the sensor. The reported design parameters in this paper are optimized values based on our extensive numerical simulations which could result in maximum sensitivity and detection limit in the proposed structure.

Sensing performance

Since the mechanism of the metamaterial absorber and the role of design parameters have been explained in detail, the influence of the surrounding medium refractive index on the absorption properties of the proposed metamaterial can be investigated. As discussed in previous sections, the absorption peaks (resonances) are related to either pure LSPR or hybrid SPP-LSPR modes. Resonance wavelength in metallic nanoparticles and nanofilms in case of LSPR or SPP mode is directly

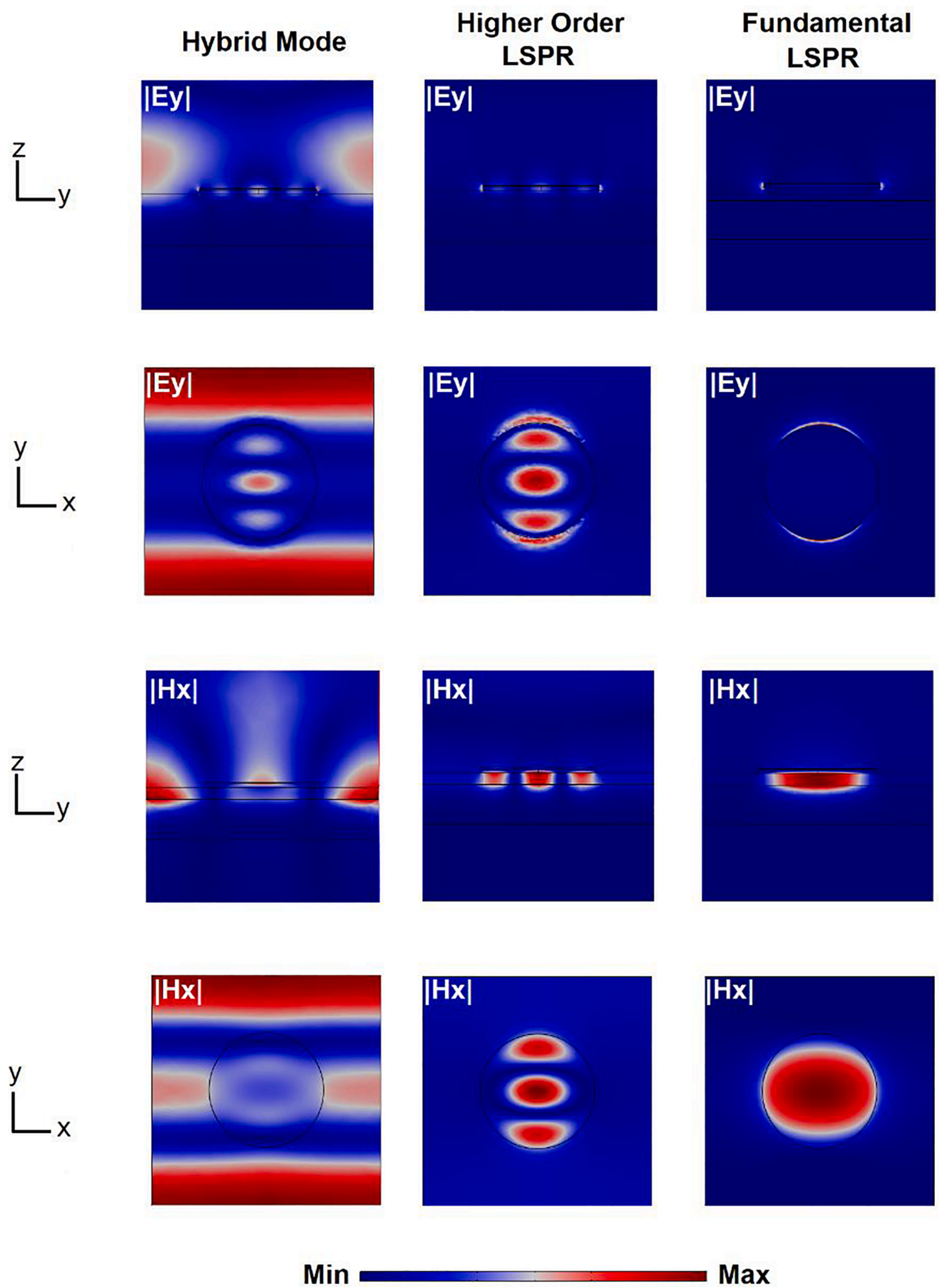

Fig. 4. The electric field |Ex| and magnetic field |Hy| distributions in the proposed graphene-assisted metamaterial absorber at three absorption peaks in the y-z, and x-y planes.

related to the refractive index (RI) of the medium that is close to the metal surface. Therefore, the ambient RI or the RI of the medium surrounding the nano-disks determines the peak wavelength (resonance wavelength) of the metamaterial. In our simulations, we observe that the absorption properties of the proposed graphene-coated metamaterial, particularly R_3, are extremely sensitive to small changes in RI value of the surrounding medium. As such, we explore the possibility of gas sensing using the proposed graphene-assisted metamaterial. We assumed that the gas medium is surrounding the graphene-coated nanodisks and model the metamaterial as radiation absorber in our FEM simulations.

In Fig. 6, we studied the variations in absorption spectra of the metamaterial while the RI of the medium increased from 1 to 1.1 in steps of 0.02. According to the data, the resonance peak of the metamaterial in IR region (R_3) redshift from 1753 nm to 1789 nm by increasing the gas RI from 1 to 1.05. We demonstrate the linear variations of resonance wavelength as a function of gas RI in Fig. 6a using a linear fit with $R^2 = 0.991$. The sensitivity (S), and the detection limit or the resolution (R) of our proposed sensor can be calculated through the following formulas:

$$S\left(\frac{nm}{RIU}\right)\frac{\Delta\lambda_{resonance}}{\Delta n}, (4)$$

$$R(RIU)\frac{\Delta n \times \Delta\lambda_{min}}{\Delta\lambda_{resonance}}, \quad (5)$$

where Δn is the difference between minimum and maximum ambient gas RI and $\Delta\lambda_{min}$ is the minimum spectral resolution of the detector. The minimum spectral resolution of detector is considered to be around 0.01 nm which is almost equal to the detection limit of high-spectral resolution spectrometers [25]. Using the above values and the peak variations in Fig. 6, the average linear sensitivity and the detection limit of

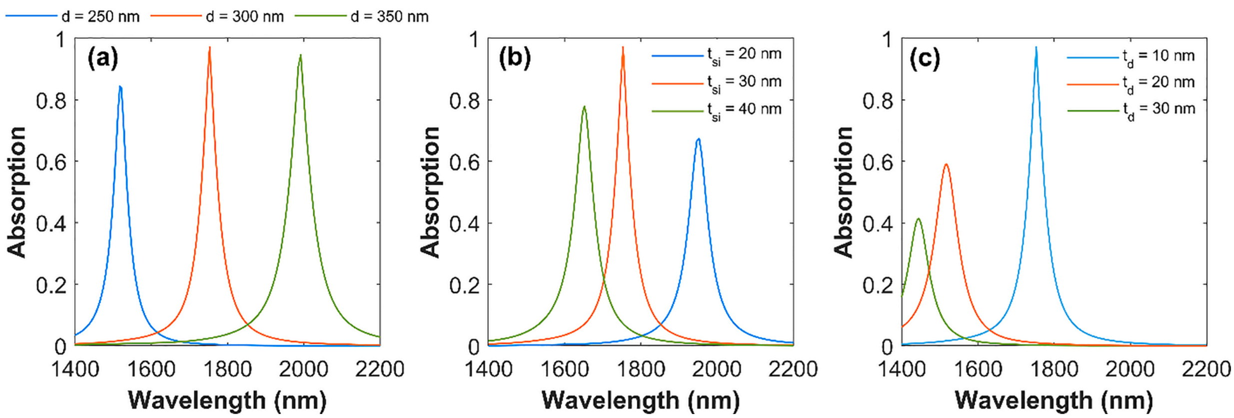

Fig. 5. The role of the design parameters of the proposed graphene-assisted metamaterial absorber on the absorption spectrum of the structure where (a) nano-disks diameter d varies between 250 nm and 350 nm, (b) thickness of SiO_2 nano-film t_{si} varies between 20 nm and 40 nm. (c) thickness of gold nano-disks t_d varies between 10 nm and 30 nm.

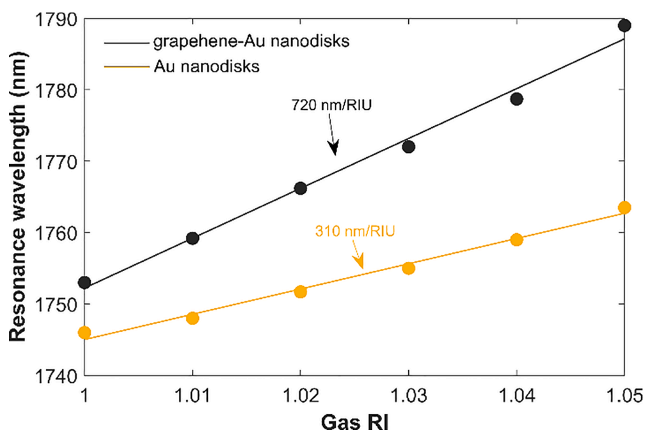

Fig. 6. Resonance wavelength of the metamaterial absorber as a function of surrounding gas RIs with and without graphene coating of the Au nano-disks. Note that the points demonstrate the simulation data points and solid lines are linear fits for the simulation data.

our proposed gas sensor, for gas RI range from 1 to 1.05, are 720 nm/RIU and approximately 1×10^{-5} RIU, respectively. This ultra-high resolution means that our proposed sensor can detect small changes in gas concentrations (for example CO_2, nitrogen and hydrogen) in various media by simply measuring the reflection or absorption spectra of the structure.

It should be noted that without graphene coating of Au nano-disks, the sensor sensitivity reduces significantly by 410 nm, from 720 nm/RIU in the case of graphene-assisted metamaterial to 310 nm/RIU in the case of Au-only metamaterial. In addition, while graphene-assisted metamaterial has a detection limit of approximately 1×10^{-5}, the metamaterial without graphene coating has a detection limit of approximately of 3×10^{-5} which may not be enough to detect small variation in gas RI. These facts highlight the significance of graphene coating in the proposed metamaterial absorber. In Table 1, we compared the performance of our proposed graphene-assisted plasmonic gas sensor to other similar plasmonic gas sensors reported in the literature.

As can be seen, our proposed graphene-assisted gas sensor has a significantly higher sensitivity compared to other reported designs of plasmonic gas sensors.

As gas concentration detection usually involves smaller RI variations around 1×10^{-3} and 1×10^{-5} (for example CO_2 detection), we also studied resonance shifts with smaller variations in RI of the surrounding medium using the proposed graphene-assisted metamaterial absorber (in steps of 10^{-3} in Fig. 7a and 10–5 in Fig. 7b). As seen in Fig. 7a, by increasing the gas RI from 1 to 1.005, the resonance wavelength shifts towards longer wavelength by 3.5 nm in a linear manner ($R^2 = 0.994$). Similarly, as demonstrated in Fig. 7b the sensor has a consistent linear response ($R^2 = 0.984$) and demonstrate a resonance wavelength change of around 0.04 nm by an increase in gas RI from 1.0004 to 1.00045 in steps of 1×10^{-5}. The reason for choosing this specific range of variations is to demonstrate the possibility of detecting low concentrations of CO_2 with our sensor as RI of CO_2 is around 1.00043 in this range [27].

The results from Fig. 7a and b means an almost 3.5 nm and 0.04 nm resonance shift per 10^{-3} and 10^{-5} RI change, respectively. These resonances shift for 10^{-3} resolution is>20 times better than that of the similar reported optical gas sensors [28], and the sensitivity of the metamaterial for 10^{-5} resolution is almost five times larger than that of the previously reported RI-based gas sensor in the literature [29]. Finally, it should also be mentioned that small variations in design parameters ($\pm$0.5 nm) due to fabrication-induced imperfections does not significantly change the sensitivity of our proposed gas sensor.

Conclusions

In summary, we proposed a new compact optical gas sensor using a plasmonic metamaterial absorber with graphene-coated gold nano-disks in the IR region. The absorption properties and gas refractive index (RI) sensitivity of the proposed metamaterial with and without graphene coating of gold nano-disks have been investigated in detail. We demonstrated that graphene coating of the gold nano-disks improves the sensitivity of the metamaterial to gas refractive index in the IR region by more than two times. We also studied the effect of the design parameters, including nano-disk diameter, nano-disk thickness and dielectric layer thickness, on the absorption properties of the metamaterial. Using the optimized design parameters, an average linear spectral sensitivity

Table 1
Performance comparison between the proposed graphene-assisted plasmonic metamaterial and recent plasmonic gas sensors.

	Plasmonic Material	Structure	Operation Region	RI Detection Range	S (nm/RIU)
Ref [6]	Graphene	Nano-gratings	Infrared	1–1.0001	430.91
Ref [26]	Gold	Nano-gratings	Visible	1–1.1	589.09
This work	Graphene on gold	Nano-disks	Infrared	1–1.05	720

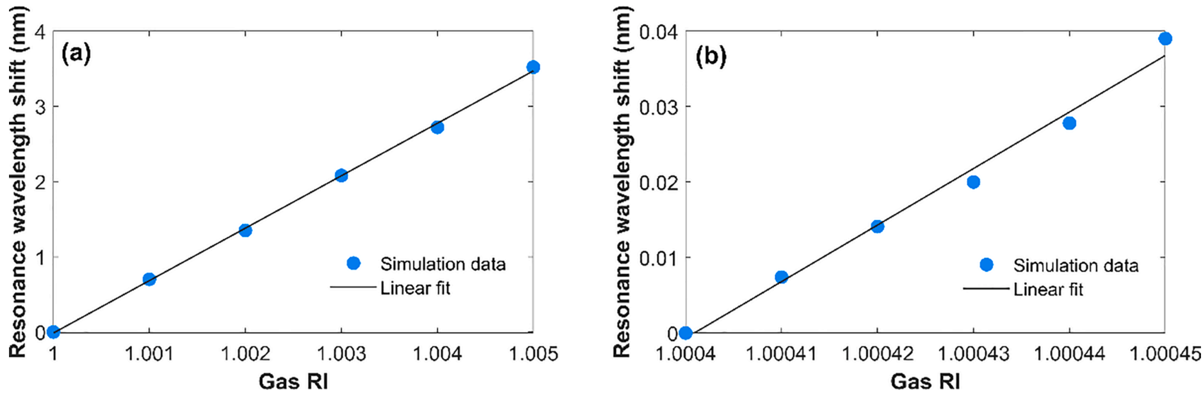

Fig. 7. Resonance wavelength shift of the graphene-assisted metamaterial as a function of Gas RI for (a) gas RI variations between 1 and 1.005, and (b) gas RI variations between 1.00040 and 1.000045.

of 720 nm/RIU and detection limit of approximately 1×10^{-5} RIU has been obtained for gas RI variations between 1 and 1.05. The proposed modality provides accurate, easy to fabricate and robust gas sensor that can be utilized in various environmental monitoring systems to detect low concentration of various gases with refractive index variations of the order of 10^{-5}.

Funding

The authors acknowledge the funding support from the Abu Dhabi award for research excellence grant (AARE-114, 2016).

Declaration of Competing Interest

The authors declare that they have no known competing financial interests or personal relationships that could have appeared to influence the work reported in this paper.

References

[1] Santhanam KSV, Ahamed NNN. Greenhouse gas sensors fabricated with new materials for climatic usage: a review. ChemEngineering 2018;2:38.
[2] Guangcan M, Cameron H, Van V. Silicon photonic dual-gas sensor for H2 and CO2 detection. Opt Express 2017;25:16250–9.
[3] Kassa-Baghdouche L. High-sensitivity spectroscopic gas sensor using optimized H1 photonic crystal microcavities. J Opt Soc Am B 2020;37:A277–84.
[4] Cody D, Naydenova I. Theoretical modeling and design of photonic structures in zeolite nanocomposites for gas sensing. Part I: surface relief gratings. J Opt Soc Am A: 2017;34:2110–9.
[5] Wijaya DR, Sarno R, Zulaika E. Gas concentration analysis of resistive gas sensor array. In: 2016 International Symposium on Electronics and Smart Devices (ISESD), Bandung, 337-342; 2016.
[6] Maleki M, Mehran M, Mokhtari A. Design of a near-infrared plasmonic gas sensor based on graphene nanogratings. J Opt Soc Am B 2020;37:3478–86.
[7] Mishra SK, Gupta BD. Surface plasmon resonance-based fiber optic chlorine gas sensor utilizing indium-oxide-doped tin oxide film. J Lightwave Technol 2015;33: 2770–6.
[8] Monfared YE, Hajati M, Liang C, Yang S, Qasymeh M. Quasi-D-shaped fiber optic plasmonic biosensor for high-index analyte detection. IEEE Sensors 2021;21(1): 17–23.
[9] Jiang L, Yuane C, Li Z, Sua J, Yia Z, Yao W, et al. Multi-band and high-sensitivity perfect absorber based on monolayer graphene metamaterial. Diam Relat Mater 2021;111:108227.
[10] Li J, Chen X, Yi Z, Yang H, Tang Y, Yiac Y, et al. Broadband solar energy absorber based on monolayer molybdenum disulfide using tungsten elliptical arrays. Mater Today Energy 2020;16:100390.
[11] Zhang Z, Chu F, Guo Z, Fan J, Li G, Cheng W. Design and optimization of surface plasmon resonance sensor based on polymer-tipped optical fiber. J Lightwave Technol 2019;37:2820–7.
[12] Li L, Liang Y, Guang J, Cui W, Zhang X, Masson J, et al. Dual Kretschmann and Otto configuration fiber surface plasmon resonance biosensor. Opt Express 2017;25: 26950–7.
[13] Frey CM, Luxenburger F, Droege S, Mackoviak V, Mizaikoff B. Near-infrared hollow waveguide gas sensors. Appl Spectrosc 2011;65:1269–74.
[14] Park J, Kodigala A, Ndao A, Kanté B. Hybridized metamaterial platform for nano-scale sensing. Opt Express 2017;25:15590–8.
[15] Ding F, Dai J, Chen Y, Zhu J, Jin Y, Bozhevolnyi SI. Broadband near-infrared metamaterial absorbers utilizing highly lossy metals. Sci Rep 2016;6:39445.
[16] Li Y, An B, Jiang S, Gao J, Chen Y, Pan S. Plasmonic induced triple-band absorber for sensor application. Opt Express 2015;23:17607–12.
[17] Zhang Y, Yia Z, Wang X, Chua P, Yao W, Zhou Z, et al. Dual band visible metamaterial absorbers based on four identical ring patches. Physica E 2021;127: 114526.
[18] Yi Z, Li J, Lin J, Qin F, Chen X, Yao W, et al. Broadband polarization-insensitive and wide-angle solar energy absorber based on tungsten ring-disc array. Nanoscale 2020;12:23077–83.
[19] Yu P, Yang H, Chen X, Yia Z, Yao W, Chen J, et al. Ultra-wideband solar absorber based on refractory titanium metal. Renewable Energy 2020;158:227–35.
[20] Hu X, Zhang Y, Chen D, Xiao X, Yu S. Design and modeling of high efficiency graphene intensity/phase modulator based on ultra-thin silicon strip waveguide. J Lightwave Technol 2019;37:2284–92.
[21] Monfared YE, Qasymeh M. Plasmonic biosensor for low-index liquid analyte detection using graphene-assisted photonic crystal fibers. Plasmonics 2021.
[22] Babar S, Weaver JH. Optical constants of Cu, Ag, and Au revisited. Appl Opt 2015; 54:477–81.
[23] Monfared YE, Ahmadian A, Dhasarathan V, Liang C. Liquid-filled highly asymmetric photonic crystal fiber sagnac interferometer temperature sensor. Photonics 2020;7, 2:33.
[24] Qasymeh M, Eleuch H. Quantum microwave-to-optical conversion in electrically driven multilayer graphene. Opt Express 2019;27:5945–60.
[25] Redding B, Liew SF, Bromberg Y, Sarma R, Cao H. Evanescently coupled multimode spiral spectrometer. Optica 2016;3:956–62.
[26] Afsheen S, Iqbal T, Aftab M, Bashir A, Tehseen A, Khan MY, et al. Modeling of 1D Au plasmonic grating as efficient gas sensor. Mater Res Express 2019;6:126203.
[27] Old JG, Gentili KL, Peck ER. Dispersion of carbon dioxide. J Opt Soc Am 1971;61: 89–90.
[28] Feng C, Feng GY, Zhou GR, Chen NJ, Zhou SH. Design of an ultracompact optical gas sensor based on a photonic crystal nanobeam cavity. Laser Phys Lett 2012;9: 875.
[29] Li K, Li J, Song Y, Fang G, Li C, Feng Z, et al. Ln slot photonic crystal microcavity for refractive index gas sensing. IEEE Photon. 2014;6(5):1–9.